Electronic Supplementary Information for

Atomic-layer-deposited ultrafine MoS₂ nanocrystals on cobalt foam for efficient and stable electrochemical oxygen evolution

Dehua Xiong,[a,b] Qingqing Zhang,[b] Wei Li,[a] Junjie Li,[a] Xiuli Fu,[c] M. F. Cerqueira,[d] Pedro Alpuim[a,d] and Lifeng Liu[a,*]

[a] *International Iberian Nanotechnology Laboratory (INL), Av. Mestre Jose Veiga, 4715-330 Braga, Portugal*

[b] *State Key Laboratory of Silicate Materials for Architectures, Wuhan University of Technology, Wuhan 430070, P. R. China*

[c] *State Key Laboratory for Information Photonics & Optical Communications, and School of Scienece, Beijing University of Posts & Telecommunications, Beijing 100876, P. R. China*

[d] *Center of Physics, University of Minho, 4710-057 Braga, Portugal*

* Corresponding author. E-mail: lifeng.liu@inl.int (L.F. Liu)

Experimental details:

Materials synthesis

All chemicals used in this work are of analytical grade and were purchased from Sigma-Aldrich. Prior to atomic layer deposition (ALD), Co foam (110 PPI, 1 mm thick) was cleaned by ultrasonication in 6 M HCl for 5 min to remove the surface oxide layer, washed sequentially in deionized (DI) water and acetone, and finally dried at 60 °C for 30 min. Subsequently, molybdenum sulfide was deposited onto the Co foam (ca. 2.8×4.0 cm^2) using a commercial ALD system (Beneq TFS-200). The deposition was carried out at 200 °C under a base pressure of ca. 1.3 mbar using $Mo(CO)_6$ (Sigma-Aldrich) and H_2S gas (99.95%, Linde) as molybdenum and sulfur sources, respectively. The $Mo(CO)_6$ container was maintained at 50 °C during deposition. The deposition sequence was as follows: 1 s exposure of $Mo(CO)_6$, 8 s dwelling, 10 s N_2 purging, followed by 1 s exposure of H_2S, 5 s dwelling, and 10 s N_2 purging. The deposition was performed for 500 and 1000 cycles to investigate the loading effect. The loading mass of $Co@MoS_2$ electrodes was determined by a high precision microbalance (Sartorius MCM36).

Characterization

The morphology, microstructure and chemical composition of $Co@MoS_2$ electrodes were examined by filed-emission scanning electron microscopy (FESEM, FEI Quanta 650) equipped with energy dispersive X-ray (EDX) spectroscopy (INCA 350, Oxford Instruments). The crystalline structure of samples was studied by X-ray diffractometry (XRD, PANalytical X'Pert PRO) using Cu K_α radiation (λ = 1.540598 Å) and a PIXcel detector. The surface chemical state was analyzed by X-ray photoelectron spectroscopy (XPS, VG Multilab 2000). Raman spectra were

collected using the WITec Alpha 300R confocal Raman system with a laser excitation wavelength of 532 nm.

Electrochemical measurements

The OER performance was evaluated using linear scan voltammetry (LSV), chronopotentiometry (CP) and electrochemical impedance spectroscopy (EIS) in a three-electrode configuration in 1.0 M KOH (pH = 13.5) with a Biologic VMP-3 potentiostat/galvanostat. A platinum wire and a saturated calomel electrode (SCE) were used as the counter and reference electrodes, respectively. The as-fabricated Co@MoS$_2$ electrode was directly used as the working electrode, and the active area was 1×1 cm^2. LSV curves were recorded at a scan rate of 5 mV s^{-1}. All current density values are normalized with respect to the geometrical surface area of the working electrode. For comparison, the electrocatalytic performance of a bare Co foam was also measured. All LSV curves measured are *iR*-corrected. The correction was done according to the following equation:

$$E_c = E_m - iR_s \qquad\qquad (1)$$

where E_c is the *iR*-corrected potential, E_m experimentally measured potential, and R_s the equivalent series resistance extracted from the EIS measurements. Unless otherwise specified, all potentials are reported versus reversible hydrogen electrode (RHE) by converting the potentials measured vs. SCE according to the following formula:
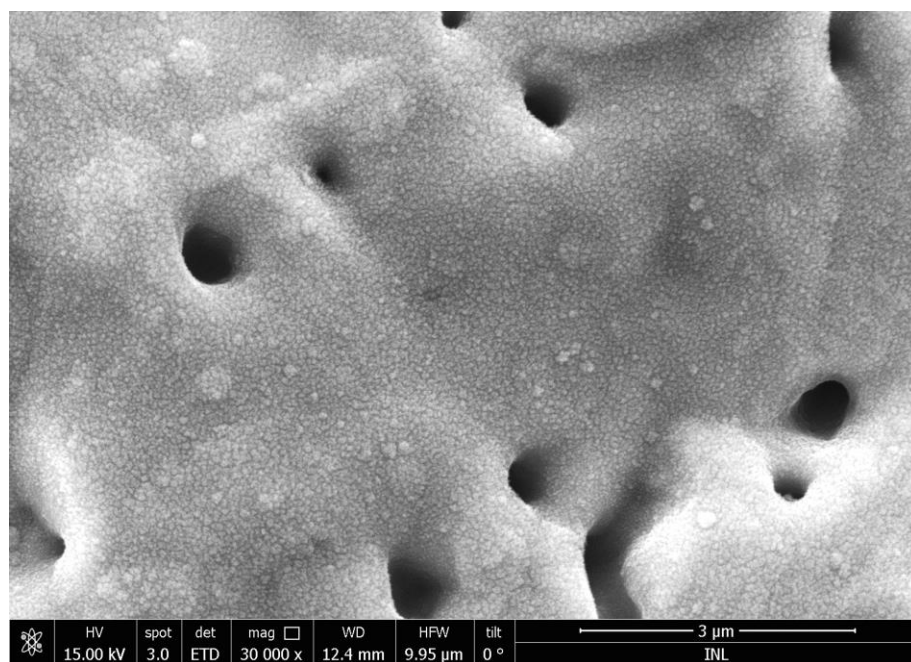
$$E (RHE) = E (SCE) + 0.241 + 0.059 \text{ pH} \qquad\qquad (2)$$

The EIS measurements were performed in the frequency range of 20 mHz – 200 kHz under a constant potential of 1.51V vs. RHE.
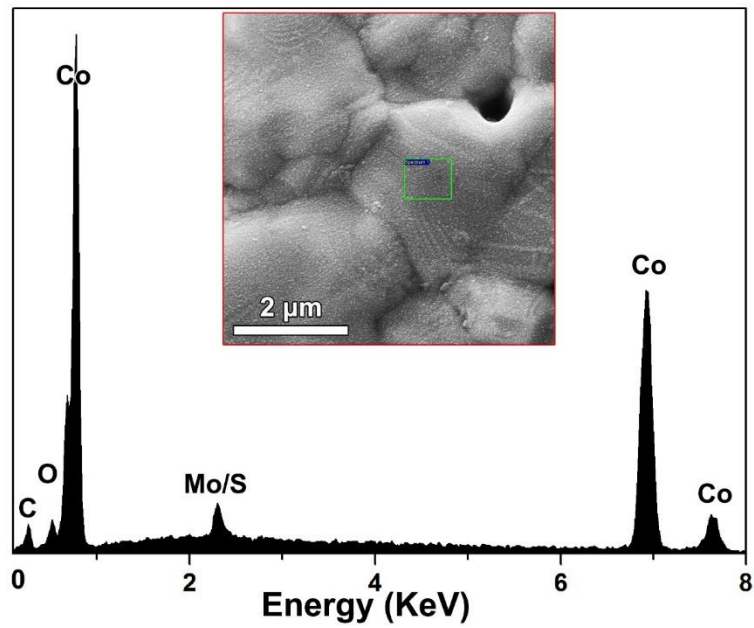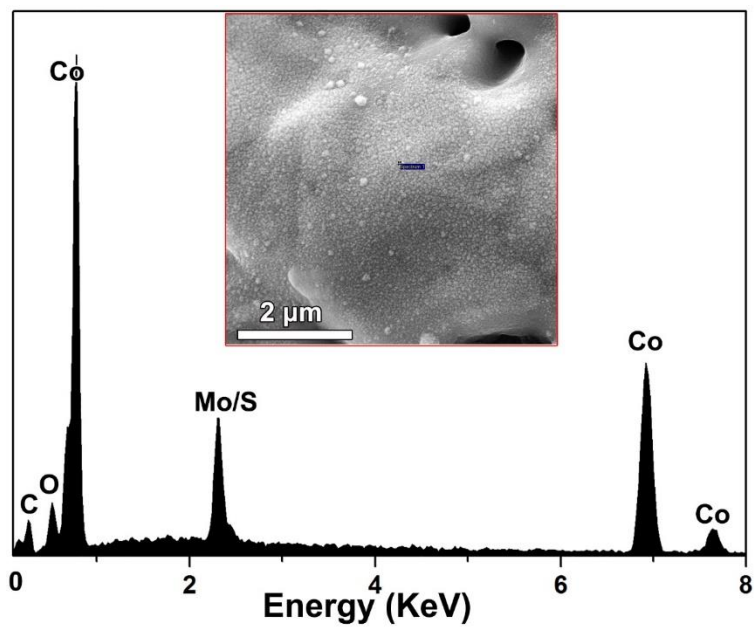
Supplementary Figures:
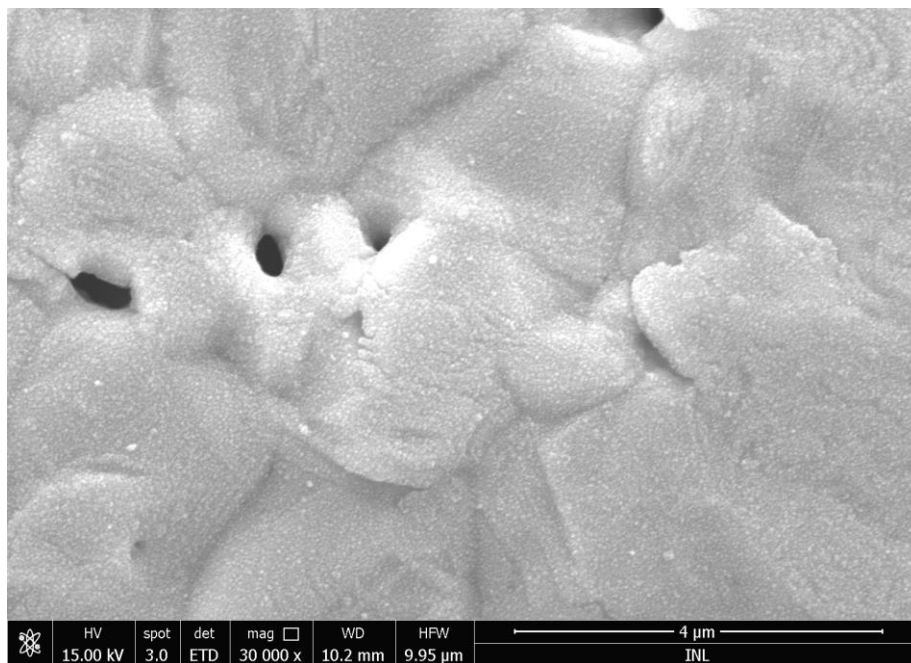
Fig. S1 SEM image of Co@MoS$_2$-500 electrodes.

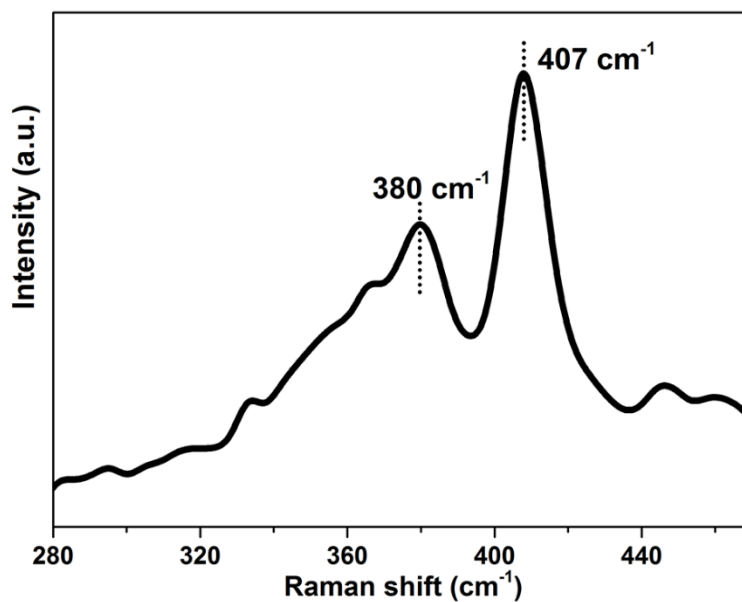**Fig. S2** SEM image of Co@MoS$_2$-1000 electrodes.

Fig. S3 SEM-EDX measurement of Co@MoS$_2$-500 electrodes.

Fig. S4 SEM-EDX measurement of Co@MoS$_2$-1000 electrodes.

Fig. S5 Digital photograph showing the appearance of glass slides before and after ALD of MoS$_2$.

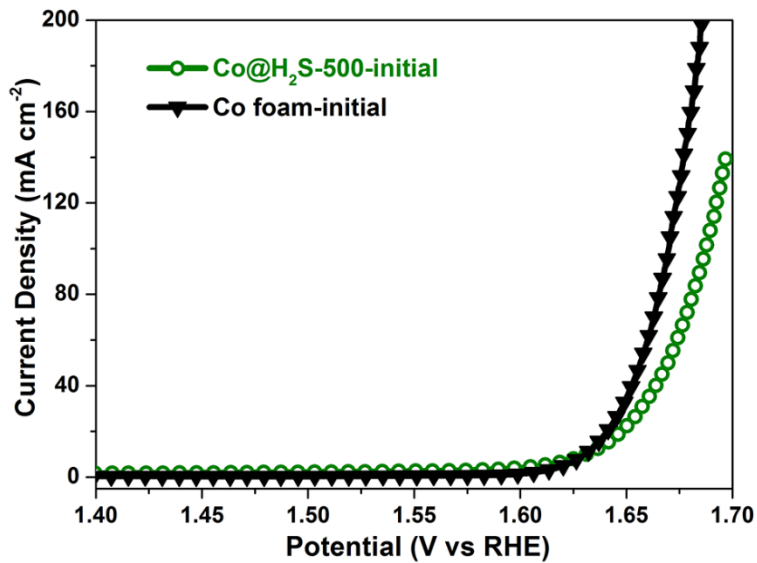**Fig. S6** Raman spectrum of Co@MoS$_2$-1000 electrode.

Fig. S7 Polarization curves of the bare Co foam and Co@H₂S-500. Scan rate: 5 mV s^{-1}.
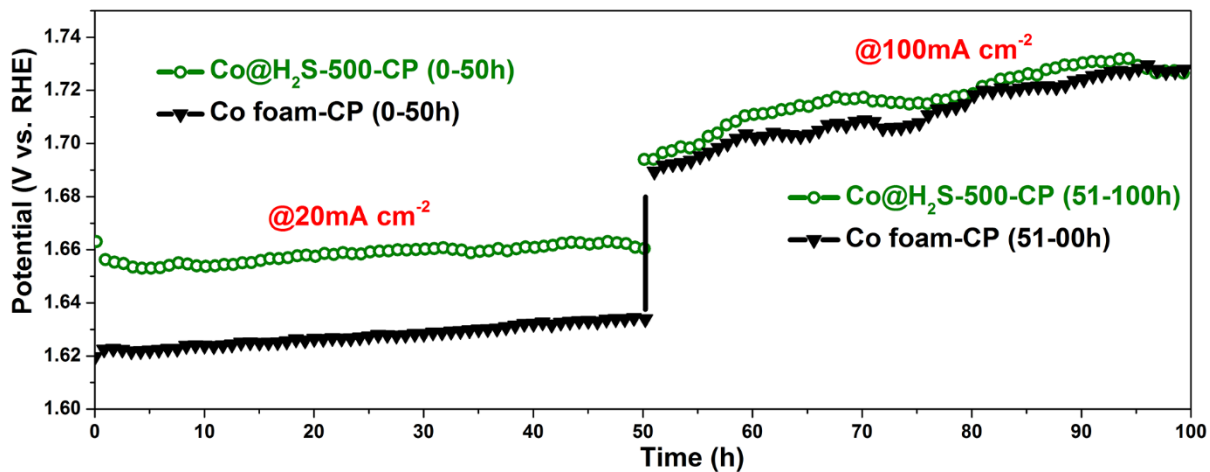
Fig. S8 Chronopotentiometric curves of the bare Co foam and Co@H₂S-500 electrodes measured at 20 mA cm^{-2} for 50 h followed by at 100 mA cm^{-2} for another 50 h.
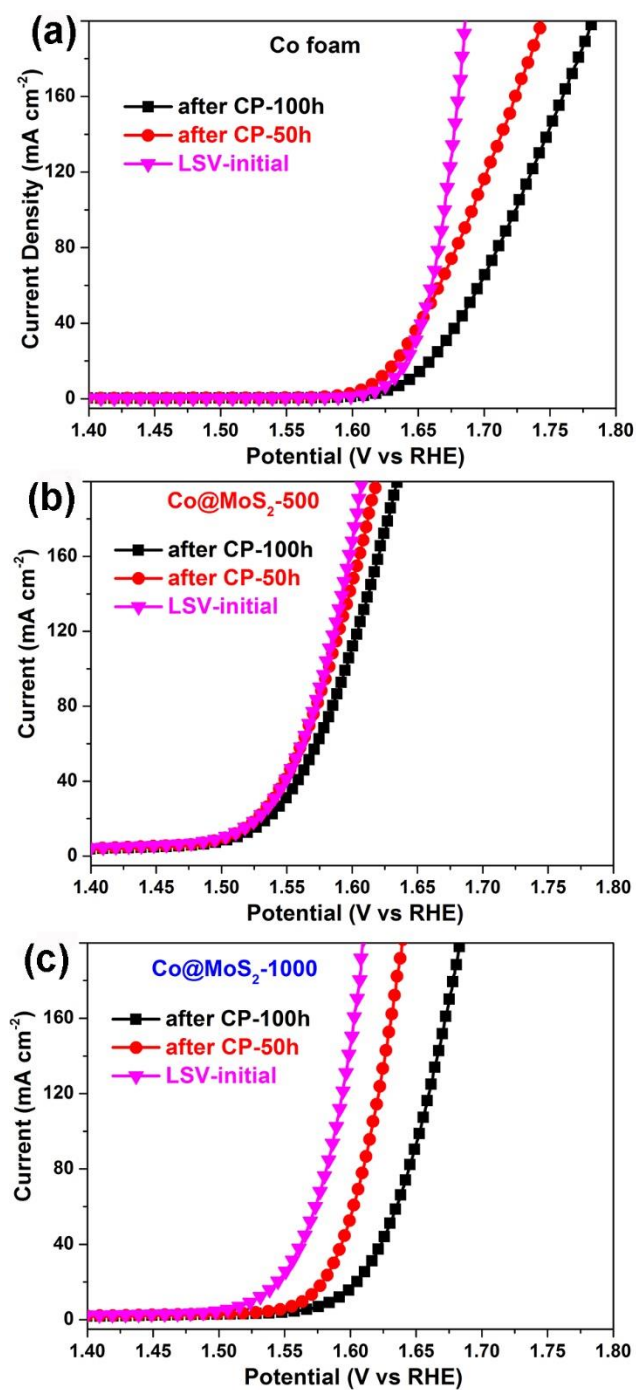
Fig. S9 *iR*-corrected polarization curves of bare Co foam, Co@MoS$_2$-500 and Co@MoS$_2$-1000 electrodes recorded before the CP test and after electrolysis at 20 mA cm^{-2} for 50 h followed by electrolysis at 100 mA cm^{-2} for another 50 h.
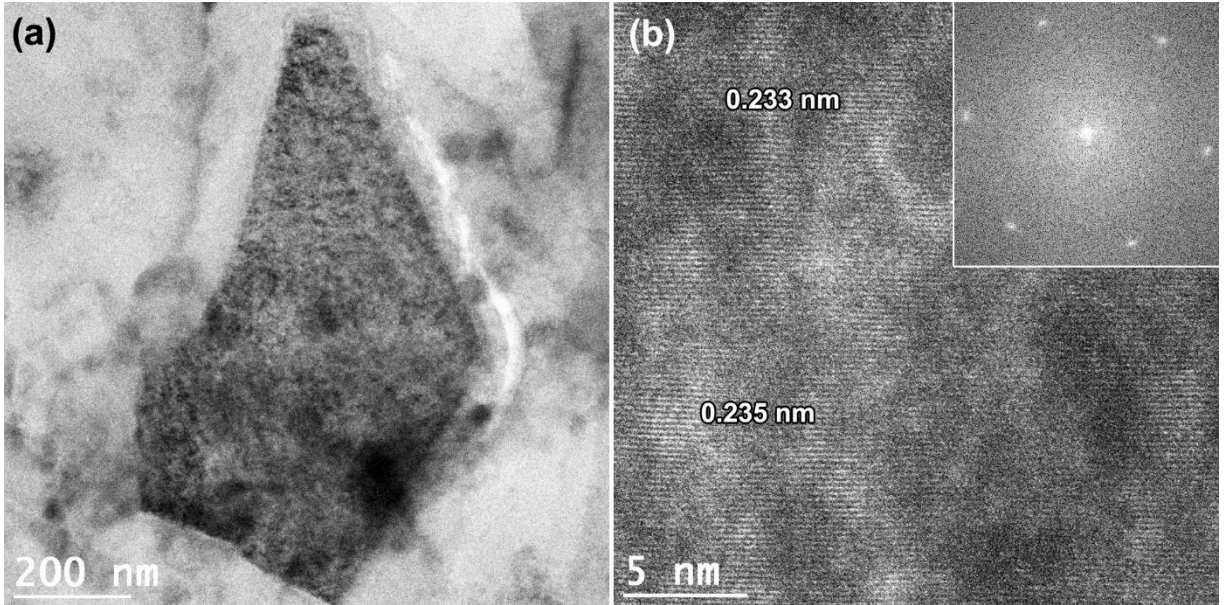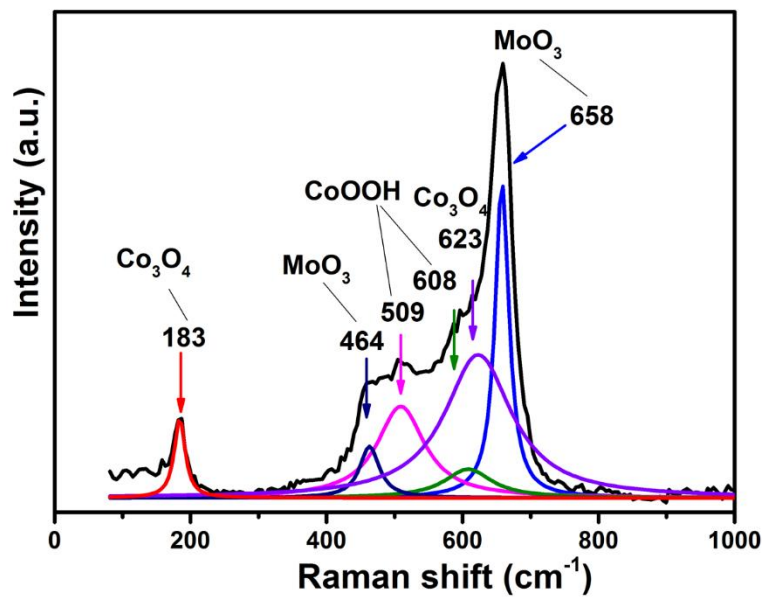
Fig. S10 (a) Low-magnification TEM and (b) HRTEM images of CoOOH nanosheets grown on bare Co foam after the extended long-term stability test under OER conditions.
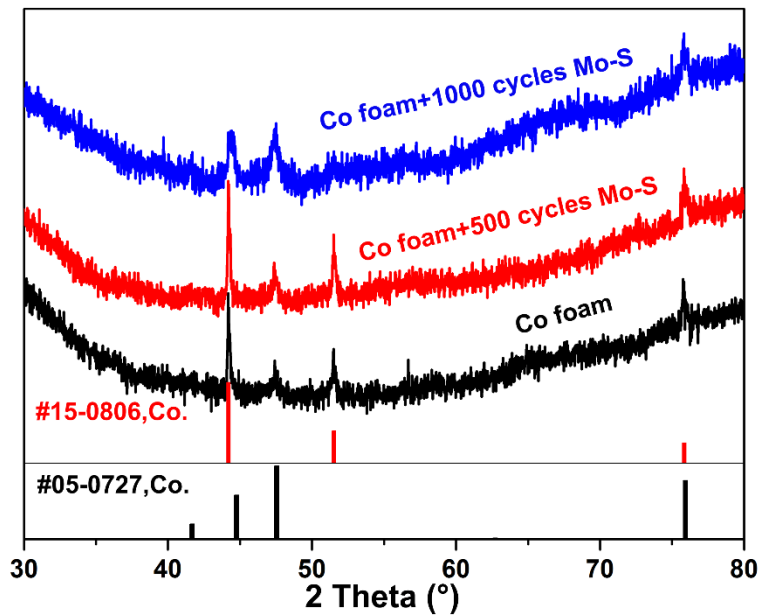
Fig. S11 XRD patterns of Co@MoS$_2$ electrodes after the 100 h galvanostatic OER test.

Fig. S12 Raman spectrum recorded from the Co@MoS$_2$-1000 electrode after the extended CP test (50 h at 20 mA cm^{-2} and another 50 h at 100 mA cm^{-2}).

Supplementary Tables

Table S1. Comparison of the OER activity of the Co@MoS$_2$ to that of noble metal as well as sulfide-based OER catalysts recently reported in the literature.

Catalysts	Electrolyte	Loading mass (mg cm^{-2})	Tafel slope (mV dec^{-1})	J$_{geo}$ (current density in mA cm^{-2} @overpotential in mV)	Reference
Co foam	1.0 M KOH	0	41	10@η=400 20@η=410	This work
Co@MoS$_2$-500		0.06	74	10@η=271 20@η=297	
Co@MoS$_2$-1000		0.09	61	10@η=296 20@η=314	
1D-RuO$_2$-CN$_x$	0.5 M KOH	0.012	56	10@η=260	ACS Appl. Mater. Interfaces, 2016, 8 (42), 28678-28688.
Commercial RuO$_2$			80	10@η=330	
IrO$_2$	1.0 M NaOH	0.8	48	10@η=380±10	J. Mater. Chem. A, 2016, 4, 3068.
RuO$_2$			65	10@η=380±20	
RuO$_2$/OCNT	0.1 M KOH	0.21	120	10@η=380	Journal of Energy Chemistry,2016, 25, 282-288.
RuO$_2$/NCNT			107	10@η=350	
IrO$_2$	0.1 M KOH	-	-	10@η~400	Anal. Chem. 2016, 88, 7597-7602.
DNA@IrO$_2$ NPs	0.1 M NaOH	-	-	10@η=312	J. Mater. Chem. A, 2015, 3, 24463-24478.
IrO$_x$	1.0 M NaOH	-	-	10@η=320	J. Am. Chem. Soc., 2013, 135 (45), 16977-16987.
Ir/Ni oxide	1.0 M KOH	0.030	44	10@η=264	ACS Appl. Mater. Interfaces, 2016, 8 (25), 15985-15990.
IrO$_x$			31	10@η=277	

Material	Electrolyte				Reference
Hollow Co_3S_4 nanosheets	0.1 M KOH	0.283	90	10@η=363	ACS Nano, 2014, 8 (10), pp 10909-10919.
Solid Co_3S_4 nanosheets			130	10@η=416	
Co_3S_4 nanosheets	0.1 M KOH	0.28	48	10@η=355	Angew. Chem. 2015, 127, 11383 -11387.
Co_3S_4 /TETA			112	10@η=430	
bulk Co_3S_4			105	10@η=590	
Co_9S_8/CNFs	1.0 M KOH	0.212	78	1@η=394 10@η=512	Adv. Mater. 2015, 27, 4752-4759.
MoS_2/CNFs			80	1@η=432	
Co_9S_8@MoS_2/CNFs			61	1@η=350 10@η=430	
MoS_2@ Nickel foam	1.0 M KOH	-	166	1@η=280	Angew. Chem. 2016, 128, 6814 -6819.
MoS_2/Ni_3S_2@ Nickel foam		9.7	88	10@η=175 10@η=218	
Co_3S_4/ex-MoS_2 hybrids	0.1 M KOH	-	36	10@η=350 10@η=290	Electrochimica Acta, 212 (2016) 890-897.
ex-MoS_2			210	-	
Co_9S_8@NC	1.0 M KOH		-	10@η=320	Dalton Trans., 2016, 45, 6352-6356.
Ni_3S_2@NC			-	10@η=390	
Co_9S_8@NC	0.1 M KOH	0.22	124	1@η=170 10@η=370	
Ni_3S_2@NC			196	1@η=300 10@η=470	
MoS_2/Nickel foam	1.0 M NaOH	-	105	20@η=310	Small, 2016, 12, 2975-2981.

Table S2. Fitting parameters for the Nyquist plots of the bare Co foam, Co@MoS$_2$-500 and Co@MoS$_2$-1000 electrodes.

Samples	R_s(Ω)	R_{sc}(Ω)	CPE1 (F cm^{-2} S^{m-1})	R_{ct} (Ω)	CPE2 (F cm^{-2} S^{m-1})
Co foam	0.521	0.519	0.892	11.31	0.044
Co@MoS$_2$-500	1.164	0.185	0.647	0.575	0.409
Co@MoS$_2$-1000	0.784	0.312	0.909	1.952	0.252